VDAC oligomers form mitochondrial pores that release small mtDNA fragments and promote lupus-like disease

Jeonghan Kim[1], **Rajeev Gupta**[2], **Luz P. Blanco**[3], **Shutong Yang**[1], **Anna Shteinfer-Kuzmine**[2], **Kening Wang**[4], **Jun Zhu**[5], **Hee Eun Yoon**[1], **Xinghao Wang**[3], **Martijn Kerkhofs**[6], **Hyeog Kang**[1], **Alexandra L. Brown**[1], **Sung-Jun Park**[1], **Xihui Xu**[1], **Eddy Zandee van Rilland**[1,#], **Myung K. Kim**[1], **Jeffrey I. Cohen**[4], **Mariana J. Kaplan**[3], **Varda Shoshan-Barmatz**[2], **Jay H. Chung**[1,*]

[1]Laboratory of Obesity and Aging Research, Genetics and Development Biology Center, National Heart Lung and Blood Institute, National Institutes of Health, Bethesda, Maryland 20892, USA

[2]Department of Life Sciences and the National Institute for Biotechnology in the Negev, Ben-Gurion University of the Negev, Beer-Sheva 84105, Israel.

[3]Systemic Autoimmunity Branch, National Institute of Arthritis and Musculoskeletal and Skin Diseases, National Institutes of Health (NIH), Bethesda, Maryland 20982, USA.

[4]Medical Virology Section, Laboratory of Infectious Diseases, National Institute of Allergy and Infectious Diseases, National Institutes of Health, Bethesda, Maryland 20892, USA.

[5]Systems Biology Center, National Heart, Lung, and Blood Institute, National Institutes of Health, Bethesda, Maryland 20892, USA.

[6]KU Leuven, Laboratory of Molecular and Cellular Signaling, Department of Cellular and Molecular Medicine and Leuven Kanker Instituut, Campus Gasthuisberg O/N-I box 802, Herestraat 49, 3000 Leuven, Belgium.

Abstract

Mitochondrial stress releases mitochondrial DNA (mtDNA) into the cytosol and triggers the type-I interferon (IFN) response. Mitochondrial outer membrane permeabilization (MOMP), which is required for mtDNA release, has been extensively studied in apoptotic cells, but little is known about MOMP in live cells. Here, we show that oxidatively stressed mitochondria release short

*Corresponding author: Jay H. Chung, chungj@nhlbi.nih.gov, (ph) 301-496-3075, (fax) 301-451-8369, Mailing address: NIH, Bldg. 10-7D14, 10 Center Dr., Bethesda, MD 20892, USA.
#Present address: BIMDC Department of Radiology, Boston Massachusetts 02215, USA.

mtDNA fragments via pores formed by the voltage-dependent anion channel (VDAC) oligomers in the mitochondrial outer membrane. Furthermore, the positively charged residues in the N-terminal domain of VDAC1 interact with mtDNA and promote VDAC1 oligomerization. The VDAC oligomerization inhibitor VBIT-4 decreases mtDNA release, IFN signaling, neutrophil extracellular traps, and disease severity in a mouse model of systemic lupus erythematosus. Thus, VDAC oligomerization inhibition is a potential therapeutic approach for diseases associated with mtDNA release.

One Sentence Summary:

Inhibiting VDAC oligomerization decreases mtDNA release, type-I interferon response, and ameliorates lupus-like disease.

Mitochondrial stress, such as that triggered by increased mitochondrial reactive oxygen species (mROS), can release mitochondrial DNA (mtDNA) into the cytosol. There, it interacts with and activates a large number of immunostimulatory DNA sensors such as cyclic GMP-AMP synthase (cGAS) that can trigger autoimmunity, including diseases caused by the type-I interferon (IFN) response (1). Mitochondrial outer membrane permeabilization (MOMP) is required for mtDNA release. To date, only BAX/BAK oligomers, which can form extremely large macropores in the mitochondrial outer membrane (MOM), have been shown to mediate mtDNA release (2–4). However, the formation of the BAX/BAK macropore generally occurs under conditions that activate BAX/BAK such as apoptosis or treatment with BAX/BAK activators (2–4). However, the pore(s) that promotes MOMP in live cells or in conditions that do not activate BAX/BAK has not been identified.

Because the voltage-dependent anion channel (VDAC) can oligomerize under oxidative stress conditions, and VDAC oligomers can form large MOM pores (5), we investigated whether VDAC could trigger MOMP in live cells and mediate mtDNA release. VDAC is the most abundant protein in MOM and regulates Ca^{2+} influx, metabolism, inflammasome activation (6) and cell death (7, 8). Moreover, the expression levels of VDAC1, the most abundant of the three VDAC isoforms, and VDAC3 are increased in the autoimmune disease systemic lupus erythematosus (SLE) (9), which, in some models, is thought to be triggered by released mtDNA (10, 11).

Previous studies on mtDNA release have used cells that are either undergoing apoptosis or that have altered mtDNA content (2, 12, 13), which make studies on the mechanism of mtDNA release difficult to interpret. To avoid these confounding variables, we studied mouse embryo fibroblasts (MEFs) deficient in endonuclease g (*Endog*), a nuclear-encoded mitochondrial endonuclease (14, 15). *Endog*$^{-/-}$ MEFs have higher levels of cytosolic mtDNA (cmtDNA) compared to WT MEFs (Fig. 1A), despite having similar levels of total mtDNA (Fig. 1B) and cellular growth rates (fig. S1A). Consistent with this, *Endog*$^{-/-}$ MEFs (Fig. 1, C and D, and fig. S1, B and C) and plasmacytoid dendritic cells (fig. S1D) have higher mRNA levels of IFN-stimulated genes (ISGs) compared to their WT counterparts. ISG expression and phosphorylation of TANK-binding kinase 1 (TBK1) and IFN regulatory factor 3 (IRF3) were significantly reduced in ρ^0 (mtDNA-deficient) cells derived from

$Endog^{-/-}$ MEFs, compared with the parental $Endog^{-/-}$ MEFs (Fig. 1, E and F, and fig. S1, E to G). Thus, the cGAS–STING pathway is activated by cmtDNA in $Endog^{-/-}$ MEFs (fig. S2, A to I). Increased mROS appears to cause the mtDNA release in $Endog^{-/-}$ MEFs because mROS was higher in $Endog^{-/-}$ MEFs (fig. S2, J and K), but the mROS scavenger mito-TEMPO decreased ISG expression in $Endog^{-/-}$ MEFs (Fig. 1G).

Under physiological conditions, tissue-culture cells are composed of two populations: live cells which make up the majority of the population and a small minority of cells undergoing spontaneous apoptosis and caspase activation. Prior studies (3, 4, 16) and our data (fig. S3A) show that activation of BAX/BAK with ABT-737 in the presence of caspase inhibition increases ISG expression. However, WT and $Bax/Bak^{-/-}$ MEFs had similar cmtDNA levels (fig. S3B), and knocking down $Endog$ robustly induced ISG expression in $Bax/Bak^{-/-}$ MEFs, albeit slightly less than that in WT MEFs (fig. S3, C and D). Thus, $Endog^{-/-}$ MOMP can occur in the absence BAX/BAK macropores. Moreover, mitochondria in $Endog^{-/-}$ MEFs tended to be slightly longer than those in WT MEFs rather than being fragmented as they would be expected with BAX/BAK activation (fig. S3E) (2, 17).

We then compared the level of apoptosis in WT and $Endog^{-/-}$ MEFs because extremely high levels of mROS can lead to apoptosis, and $Endog^{-/-}$ MEFs have higher mROS compared to WT MEFs (fig. S2, J and K). WT and $Endog^{-/-}$ MEFs had similar levels of apoptotic indicators such as caspase activity (fig. S3F), cell viability (fig. S3G), lactate dehydrogenase (LDH) release (fig. S3H), and ethidium homodimer-1 (EthD-1) staining (fig. S3I) either before or after the induction of apoptosis by BAX/BAK. Thus, $Endog^{-/-}$ MEFs have levels of mROS stress high enough to promote MOMP and mtDNA release in a BAX/BAK-independent manner but insufficient to promote apoptosis at the cellular level (fig. S3I).

An alternative mediator of MOMP may be VDAC, and indeed, $Vdac1^{-/-}$, $Vdac3^{-/-}$, and $Vdac1/3^{-/-}$ MEFs had lower levels of ISG mRNA and cmtDNA compared to WT MEFs (Fig. 2, A and B, and fig. S4, A to C) despite having similar total mtDNA levels (fig. S4D). We excluded VDAC2 from our study because VDAC2-deficiency promotes apoptosis (8). Additionally, a knock down of $Endog$ increased ISG expression in WT and $Bax/Bak^{-/-}$ MEFs, but not in $Vdac1/3^{-/-}$ MEFs (Fig. 2C and fig. S3C) and treatment with the VDAC inhibitor DIDS (18) decreased ISG expression in $Endog^{-/-}$ MEFs (fig. S4E). In agreement with their reduced type-I IFN signaling, $Vdac1/3^{-/-}$ MEFs were less resistant to HSV-1 infection compared to WT MEFs (fig. S4, F to H). Thus, both VDAC1 and VDAC3 contribute to both MOMP and mtDNA release.

VDAC does not promote mtDNA release by increasing the subpopulation of cells undergoing apoptosis as the total caspase activity was not altered in $Vdac1/3^{-/-}$ MEFs even in the presence of a moderate concentration of H_2O_2 (fig. S5A), which increases cmtDNA (Fig. 2B). In contrast, BAX/BAK, but not VDAC1/3, was required for ABT-737-induced apoptosis (fig. S5B), indicating that in the presence of BAX/BAK macropores (e.g. apoptosis), VDAC is not required to drive MOMP (fig. S5C).

We initially hypothesized that VDAC regulates mtDNA release by promoting Ca^{2+} influx (19), which opens the mitochondrial permeability transition pore (mPTP) in the

mitochondrial inner membrane (MIM) in a manner that does not trigger apoptosis at the whole cell level (20, 21). This would be possible only if the population of affected mitochondria is very small so that the total caspase activity remains near background levels. Chelation of Ca^{2+} with BAPTA decreased ISG expression (fig. S6, A to C), and inhibiting mPTP opening with cyclosporin A (CsA) decreased mtDNA release in both $Endog^{-/-}$ MEFs and WT mitoplasts as well as ISG mRNA levels in $Endog^{-/-}$ MEFs (fig. S6, D to F). However, mtDNA release from mitochondria deficient in mitochondrial calcium uptake 1 (MICU1), which had elevated mROS levels and IFN responses (fig. S6, G to I) (22), was still inhibited by DIDS in the absence of Ca^{2+} (fig. S6J). Thus, VDAC may play a Ca^{2+} flux-independent role in mtDNA release. In agreement with this, the highly potent VDAC1 oligomerization inhibitor VBIT-4 (23) decreased cmtDNA levels and ISG expression in $Endog^{-/-}$ MEFs (Fig. 2, D and E), without inhibiting either Ca^{2+} uptake (fig. S6K) or mPTP opening (fig. S6L) in the mitochondria. We then loaded mtDNA fragments into liposomes with or without membrane-reconstituted VDAC1. The presence of VDAC1 in liposomes increased mtDNA passage across the lipid membrane (Fig. 2F), but VBIT-4 decreased VDAC1 oligomerization (fig. S7, A and B) as well as mtDNA efflux (Fig. 2F). Thus, VDAC1 oligomers are sufficient to permeabilize lipid membranes for mtDNA passage.

As the intact mtDNA is large (16–17 kb) and is tethered to the MIM in nucleoid complexes (24), we hypothesized that short and free (untethered) intra-mtDNA fragments (fimtDNA) that can pass through VDAC oligomer pores pre-exist in living cells (fig. S8A). To investigate this possibility, we treated mitochondria purified from WT MEFs with cytoskeleton (CSK) buffer, which gently permeabilizes mitochondrial membranes and releases fimtDNA while leaving mitochondrial nucleoids intact (24). Interestingly, the sequences corresponding to a region within the D-loop in the mitochondrial genome were over represented in the fimtDNA pool (fig. S8, A and B). A size distribution analysis excluding the sequences with 100% homology to both mitochondrial and nuclear genomes indicated that the peak sizes of fimtDNA and cmtDNA are almost identical (~110 bp) (Fig. 2G). Treatment of WT MEFs with mito-TEMPO (fig. S8C) or the mTORC1 inhibitor everolimus (fig. S8D), which promotes mitophagy and elimination of damaged mitochondria, decreased fimtDNA. Thus, fimtDNA accumulates preferentially within a subpopulation of mitochondria with elevated mROS, and cmtDNA is derived largely from fimtDNA in live cells (fig. S5C).

Studies with planar lipid bilayer (PLB) reconstituted with VDAC1 indicate that the N-terminal domain of VDAC1 can interact directly with mtDNA (fig. S9). The N-terminal domain, which is evolutionarily conserved (fig. S10A), is hydrophilic and is thought to translocate out of the channel when VDAC1 is in an oligomerized state (Fig. 3A) (25). This raises the possibility that the negatively charged backbone of mtDNA may interact with multiple VDAC1 molecules simultaneously and act as a scaffold to stabilize the oligomers (Fig. 3A). Indeed, mtDNA increased the formation of VDAC1 trimers and higher order oligomers (Fig. 3, B and C) in vitro. In agreement with higher cmtDNA in $Endog^{-/-}$ MEFs (Fig. 1A), co-immunoprecipitation with anti-VDAC1 antibody pulled down more mtDNA in $Endog^{-/-}$ MEFs compared to WT MEFs (Fig. 3D). VDAC1 oligomerization was also increased in $Endog^{-/-}$ MEFs compared to WT MEFs, but it was reduced by the elimination of mtDNA in $Endog^{-/-}$ MEFs (ρ^0) (Fig. 3, E and F). In contrast, BAK oligomerization was

not increased in $Endog^{-/-}$ MEFs (Fig. 3G), and BAI, the BAX oligomerization inhibitor (26), did not reduce ISG expression in $Endog^{-/-}$ MEFs (Fig. 3H). Thus, mtDNA may promote further VDAC1 oligomerization, creating a feed-forward cycle.

The N-terminal domain of VDAC1 contains three positively charged residues (K12, R15, K20) that could interact with the negatively charged backbone of mtDNA (Fig. 3I). Indeed, mtDNA fragments were pulled down by a 26 a.a. VDAC1 N-terminal peptide but not by a VDAC1 N-terminal mutant peptide (3A) in which K12, R15, K20 residues were replaced by Ala (A) (Fig. 3J). We then examined H_2O_2-induced expression of ISG in $Vdac1/3^{-/-}$ MEFs with restored expression of either WT VDAC1, the 3A-mutant VDAC1, or ΔN-terminal VDAC1 (fig. S10B). ISG expression was reduced in MEFs expressing either the 3A-mutant VDAC1 (Fig. 3K) or ΔN-terminal VDAC1 (fig. S10C), compared with those expressing WT VDAC1. Thus, direct mtDNA–VDAC interactions appear to promote VDAC oligomerization and increase mtDNA release.

An excessive type-I IFN response is a hallmark of SLE (27). Gene Expression Omnibus (GEO) analysis revealed increased mRNA expression of *VDAC1/3* and decreased expression of *ENDOG* in SLE patients (fig. S11A) (9). However, mRNA levels of *BAK, BAX, VDAC2*, and *HSP60* were not changed in SLE patients (fig. S11A). These findings, combined with the observation that type-I IFN responses in *Endog*-knock down MEFs were VDAC(1 and 3)-dependent (Fig. 2C), suggest that VDAC oligomerization may be associated with SLE. Indeed, splenocytes from MpJ-*Fas^lpr* lupus-prone mice had more VDAC1 oligomers than MpJ control mice (Fig. 4A and fig. S11B) as did peripheral blood mononuclear cells (PBMCs) from SLE patients compared to healthy controls (Fig. 4B and fig. S11C). Splenocytes from MpJ-*Fas^lpr* mice also had elevated cmtDNA compared to those from MpJ mice, but this was abrogated with VBIT-4 treatment (Fig. 4C).

We next investigated whether VBIT-4 could ameliorate lupus-like symptoms in MpJ-*Fas^lpr* mice. VBIT-4 blocked the development of skin lesions and the thickening of the epidermis that accompanies leukocyte infiltration, and suppressed facial and dorsal alopecia without affecting mortality or body weight (fig. S12, A to C). VBIT-4 also decreased spleen and lymph node weights (fig. S12D). Furthermore, the levels of ISG mRNA (fig. S12E), renal immune complex deposition (Fig. 4, E and D), proteinuria (Fig. 4F), anti-dsDNA antibody (Fig. 4G), antinuclear antibody (ANA) (Fig. 4H), IgG (Fig. 4I), and cell-free mtDNA (Fig. 4J) were all reduced by VBIT-4. Cell-free mtDNA plays an immunostimulatory role in human and mouse SLE (10, 11). A potential source of cell-free mtDNA in MpJ-*Fas^lpr* mice is neutrophil extracellular traps (NETs), in a cell-death process called NETosis (11). mROS is an important trigger for NETosis (11), and VBIT-4 decreased mROS in neutrophils as well as other immune cells from SLE patients (Fig. 4K and fig. S12F). In agreement with this, VBIT-4 suppressed NETosis in low-density granulocytes (LDGs), a distinct class of pro-inflammatory and NETosis-prone neutrophils from SLE patients, and normal-density granulocytes (NDGs) isolated from SLE patients and healthy controls (Fig. 4L and fig. S12G). Thus, VDAC oligomerization increases mROS and NETosis, proposed important triggers of autoimmunity, in both human neutrophils (healthy and SLE) and during lupus-like disease in mice (fig. S12H).

In conclusion, we propose that the MOM pore that mediates mtDNA release and type-I IFN response depends on the level of mitochondrial stress: oligomerized VDAC1 for moderate-level stress and BAX/BAK macropores for extreme-level stress and/or apoptosis (fig. S13). It should be noted that there are other pathways of mtDNA release (10) and that SLE is a very heterogenous disease. Nevertheless, inhibiting VDAC oligomerization may be an alternate therapeutic approach for a wide-range of diseases, like SLE and Parkinson's disease (28), that are thought to be associated with mtDNA release.

Supplementary Material

Refer to Web version on PubMed Central for supplementary material.

Acknowledgements

## Data and materials availability:

All other data and materials are available from the corresponding author upon request. Gene Expression Omnibus (GEO) database of human SLE patient is supported by national center for biotechnology information (GEO accession number: GSE13887).

References and Notes

1. West AP, Shadel GS, Mitochondrial DNA in innate immune responses and inflammatory pathology. Nat Rev Immunol 17, 363–375 (2017). [PubMed: 28393922]

2. McArthur K et al., BAK/BAX macropores facilitate mitochondrial herniation and mtDNA efflux during apoptosis. Science 359, (2018).

3. Rongvaux A et al., Apoptotic caspases prevent the induction of type I interferons by mitochondrial DNA. Cell 159, 1563–1577 (2014). [PubMed: 25525875]

4. White MJ et al., Apoptotic caspases suppress mtDNA-induced STING-mediated type I IFN production. Cell 159, 1549–1562 (2014). [PubMed: 25525874]

5. Keinan N, Tyomkin D, Shoshan-Barmatz V, Oligomerization of the mitochondrial protein voltage-dependent anion channel is coupled to the induction of apoptosis. Mol Cell Biol 30, 5698–5709 (2010). [PubMed: 20937774]

6. Zhou R, Yazdi AS, Menu P, Tschopp J, A role for mitochondria in NLRP3 inflammasome activation. Nature 469, 221–225 (2011). [PubMed: 21124315]

7. Shoshan-Barmatz V, Krelin Y, Shteinfer-Kuzmine A, VDAC1 functions in Ca(2+) homeostasis and cell life and death in health and disease. Cell Calcium 69, 81–100 (2018). [PubMed: 28712506]

8. Cheng EH, Sheiko TV, Fisher JK, Craigen WJ, Korsmeyer SJ, VDAC2 inhibits BAK activation and mitochondrial apoptosis. Science 301, 513–517 (2003). [PubMed: 12881569]

9. Fernandez DR et al., Activation of mammalian target of rapamycin controls the loss of TCRzeta in lupus T cells through HRES-1/Rab4-regulated lysosomal degradation. J Immunol 182, 2063–2073 (2009). [PubMed: 19201859]

10. Caielli S et al., Oxidized mitochondrial nucleoids released by neutrophils drive type I interferon production in human lupus. J Exp Med 213, 697–713 (2016). [PubMed: 27091841]

11. Lood C et al., Neutrophil extracellular traps enriched in oxidized mitochondrial DNA are interferogenic and contribute to lupus-like disease. Nat Med 22, 146–153 (2016). [PubMed: 26779811]

12. Nakahira K et al., Autophagy proteins regulate innate immune responses by inhibiting the release of mitochondrial DNA mediated by the NALP3 inflammasome. Nat Immunol 12, 222–230 (2011). [PubMed: 21151103]

13. West AP et al., Mitochondrial DNA stress primes the antiviral innate immune response. Nature 520, 553–557 (2015). [PubMed: 25642965]

14. Schafer P et al., Structural and functional characterization of mitochondrial EndoG, a sugar non-specific nuclease which plays an important role during apoptosis. J Mol Biol 338, 217–228 (2004). [PubMed: 15066427]

15. McDermott-Roe C et al., Endonuclease G is a novel determinant of cardiac hypertrophy and mitochondrial function. Nature 478, 114–118 (2011). [PubMed: 21979051]

16. Ichim G et al., Limited mitochondrial permeabilization causes DNA damage and genomic instability in the absence of cell death. Mol Cell 57, 860–872 (2015). [PubMed: 25702873]

17. Riley JS et al., Mitochondrial inner membrane permeabilisation enables mtDNA release during apoptosis. EMBO J 37, (2018).

18. Ben-Hail D, Shoshan-Barmatz V, VDAC1-interacting anion transport inhibitors inhibit VDAC1 oligomerization and apoptosis. Biochim Biophys Acta 1863, 1612–1623 (2016). [PubMed: 27064145]

19. Baines CP, Kaiser RA, Sheiko T, Craigen WJ, Molkentin JD, Voltage-dependent anion channels are dispensable for mitochondrial-dependent cell death. Nat Cell Biol 9, 550–555 (2007). [PubMed: 17417626]

20. Garcia N, Chavez E, Mitochondrial DNA fragments released through the permeability transition pore correspond to specific gene size. Life Sci 81, 1160–1166 (2007). [PubMed: 17870132]

21. Patrushev M et al., Mitochondrial permeability transition triggers the release of mtDNA fragments. Cell Mol Life Sci 61, 3100–3103 (2004). [PubMed: 15583871]

22. Liu JC et al., MICU1 Serves as a Molecular Gatekeeper to Prevent In Vivo Mitochondrial Calcium Overload. Cell Rep 16, 1561–1573 (2016). [PubMed: 27477272]

23. Ben-Hail D et al., Novel Compounds Targeting the Mitochondrial Protein VDAC1 Inhibit Apoptosis and Protect against Mitochondrial Dysfunction. J Biol Chem 291, 24986–25003 (2016). [PubMed: 27738100]

24. Iborra FJ, Kimura H, Cook PR, The functional organization of mitochondrial genomes in human cells. BMC Biol 2, 9 (2004). [PubMed: 15157274]

25. Geula S, Ben-Hail D, Shoshan-Barmatz V, Structure-based analysis of VDAC1: N-terminus location, translocation, channel gating and association with anti-apoptotic proteins. Biochem J 444, 475–485 (2012). [PubMed: 22397371]

26. Garner TP et al., Small-molecule allosteric inhibitors of BAX. Nat Chem Biol 15, 322–330 (2019). [PubMed: 30718816]

27. Obermoser G, Pascual V, The interferon-alpha signature of systemic lupus erythematosus. Lupus 19, 1012–1019 (2010). [PubMed: 20693194]

28. Sliter DA et al., Parkin and PINK1 mitigate STING-induced inflammation. Nature 561, 258–262 (2018). [PubMed: 30135585]
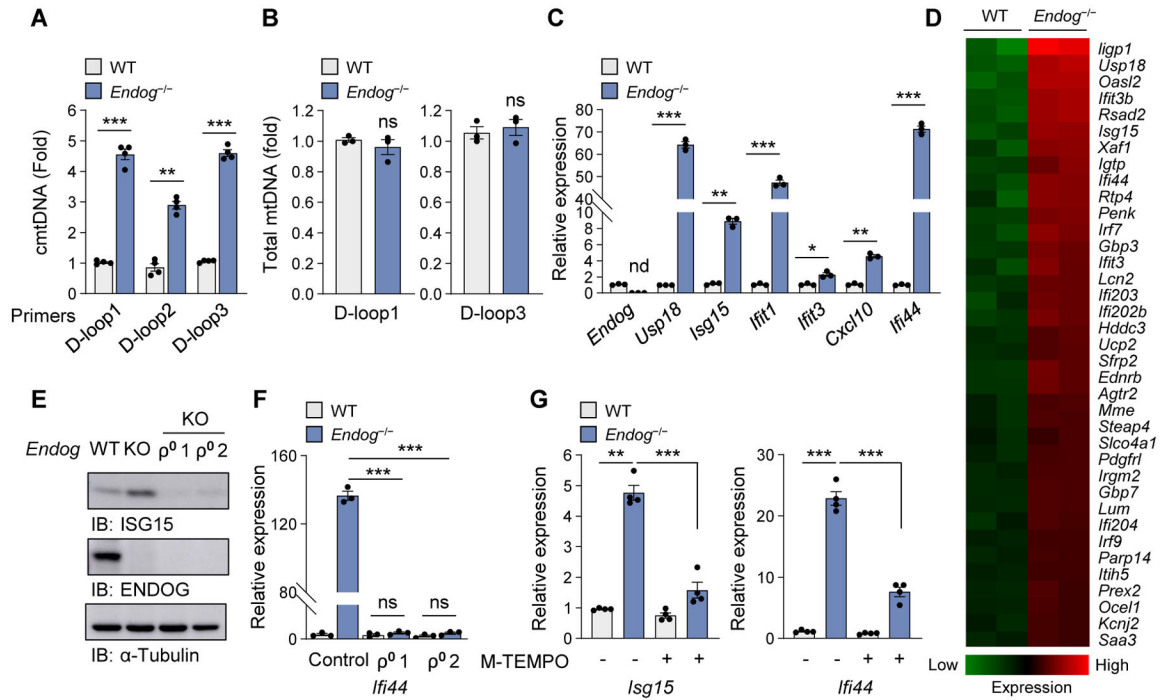
**Fig. 1. *Endog*-deficiency increases cmtDNA and type-I IFN signaling.**

(**A** and **B**) Quantification of cmtDNA (A) and total mtDNA (B) in WT and *Endog*$^{-/-}$ MEFs. (**C** and **D**) ISG expression levels (C) and heat map analysis of RNAseq data (D) in WT and *Endog*$^{-/-}$ MEFs. (**E** and **F**) ISG expression levels in WT and *Endog*$^{-/-}$ MEFs as well as two independently generated ρ^0 MEFs (ρ^0 1 and ρ^0 2) were determined by immunoblotting (E) and RT-qPCR (F). (**G**) ISG expression was measured in WT and *Endog*$^{-/-}$ MEFs after treatment with Mito(M)-TEMPO (10 μM) for 48 h. All values are presented as the mean ± SEM of at least three independent experiments. *p < 0.05; **p < 0.01; ***p < 0.005; nd, not detected; ns, not significant.
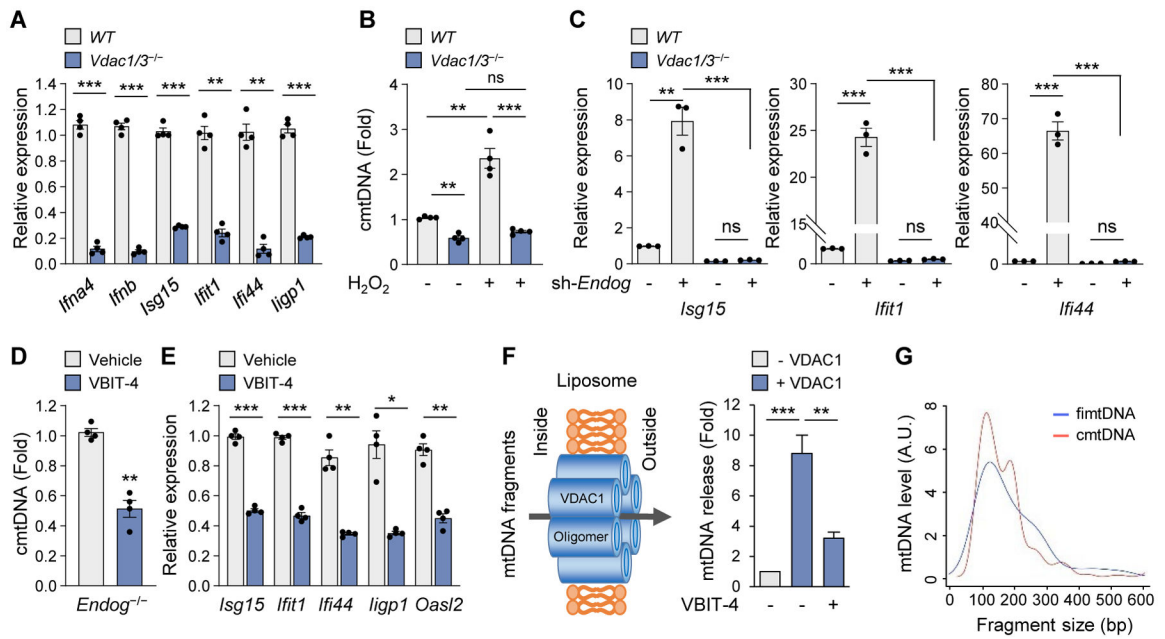
Fig. 2. VDAC oligomerization is required for mtDNA fragment release.
(**A**) ISG expression levels in WT and *Vdac1/3$^{-/-}$* MEFs. (**B**) cmtDNA levels were determined in WT and *Vdac1/3$^{-/-}$* MEFs after treatment with H$_2$O$_2$ (100 μM) for 18 h. (**C**) ISG expression levels were measured in WT and *Vdac1/3$^{-/-}$* MEFs after knocking down *Endog*. (**D** and **E**) cmtDNA (D) and ISG expression (E) levels were measured after treatment with VBIT-4 (10 μM) in *Endog$^{-/-}$* MEFs. (**F**) VDAC1 oligomerization-dependent release of mtDNA from mtDNA-loaded liposomes and inhibition by VBIT-4. (**G**) Fragment-size distribution of the fimtDNA and cmtDNA. All values are presented as the mean ± SEM of at least three independent experiments. *p < 0.05; **p < 0.01; ***p < 0.005; ns, not significant.
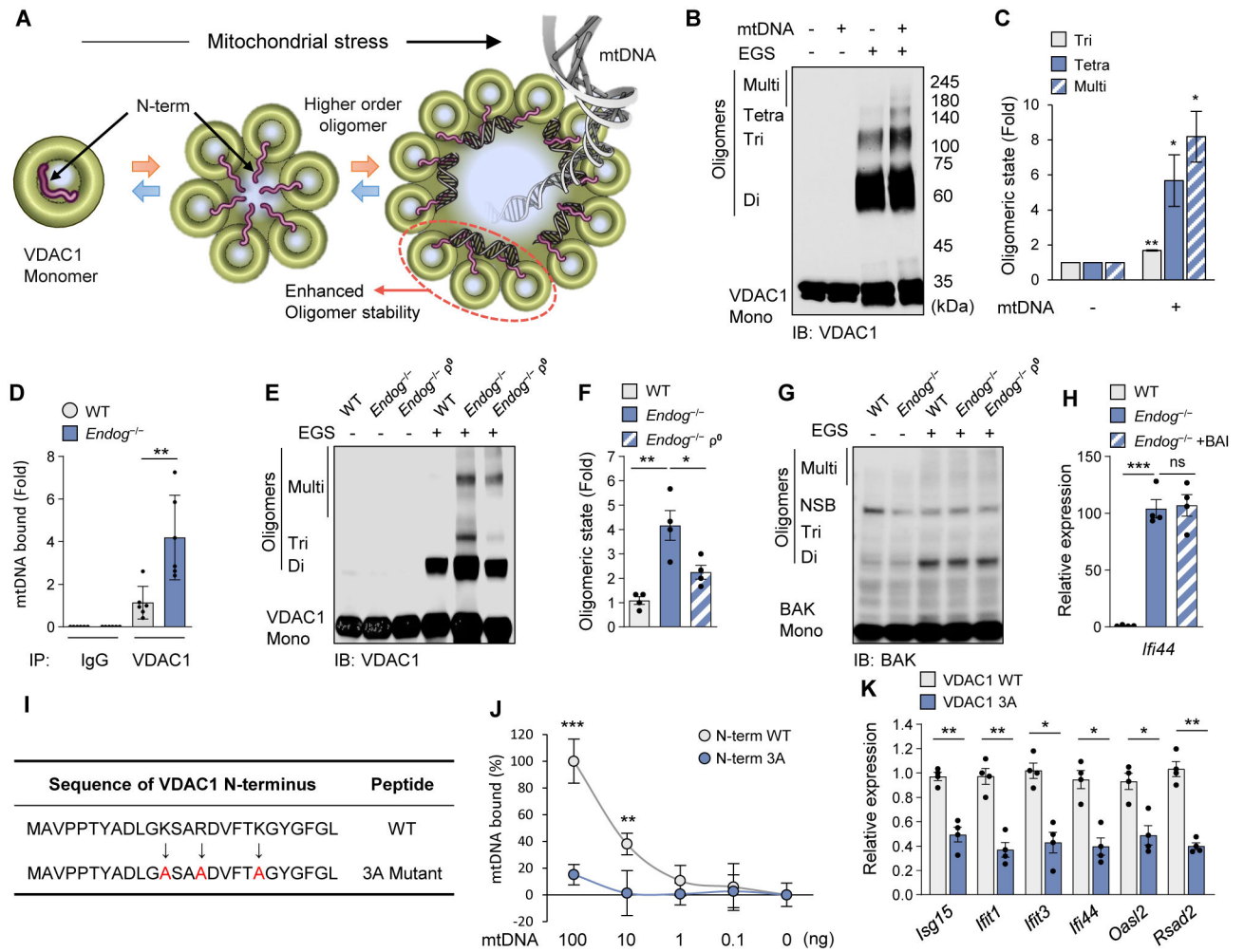
Fig. 3. mtDNA interacts with VDAC1 and stabilizes its oligomeric state.
(**A**) Schematic diagram of VDAC1 oligomerization accompanied by the N-terminal domain (red) translocation into the large oligomer pore. We could not characterize VDAC3 in vitro because it tends to form aggregates. (**B** and **C**) mtDNA-induced oligomerization of purified VDAC1 was visualized by immunoblotting after treatment with the cross-linking reagent EGS to stabilize the oligomers during electrophoresis (B). Quantitative analysis of oligomers is shown (C). (**D**) mtDNA binding to VDAC1 in WT and *Endog*$^{-/-}$ MEFs. (**E** to **G**) VDAC1 (E) and BAK (G) oligomerization in WT, *Endog*$^{-/-}$ and *Endog*$^{-/-}$ ρ^0 MEFs was visualized by immunoblotting. The positions of VDAC1 monomers (Mono), dimers (Di), trimers (Tri) and multimers (Multi) are indicated. NSB, non-specific band. Quantitative analysis of VDAC1 oligomers is shown (F). (**H**) ISG expression was measured in WT and *Endog*$^{-/-}$ MEFs after treatment with the BAX oligomerization inhibitor (BAI) (2 μM) for 24 h. (**I**) The amino-acid sequence of the VDAC1 N-terminal peptide. The positively charged amino acids were mutated to alanine (A: red color). (**J**) Direct interaction of mtDNA fragments with WT and 3A N-terminal 26 amino-acid peptides. (**K**) ISG expression levels were measured by RT-qPCR after H_2O_2 (100 μM) treatment for 18 h in MEFs expressing either WT or 3A
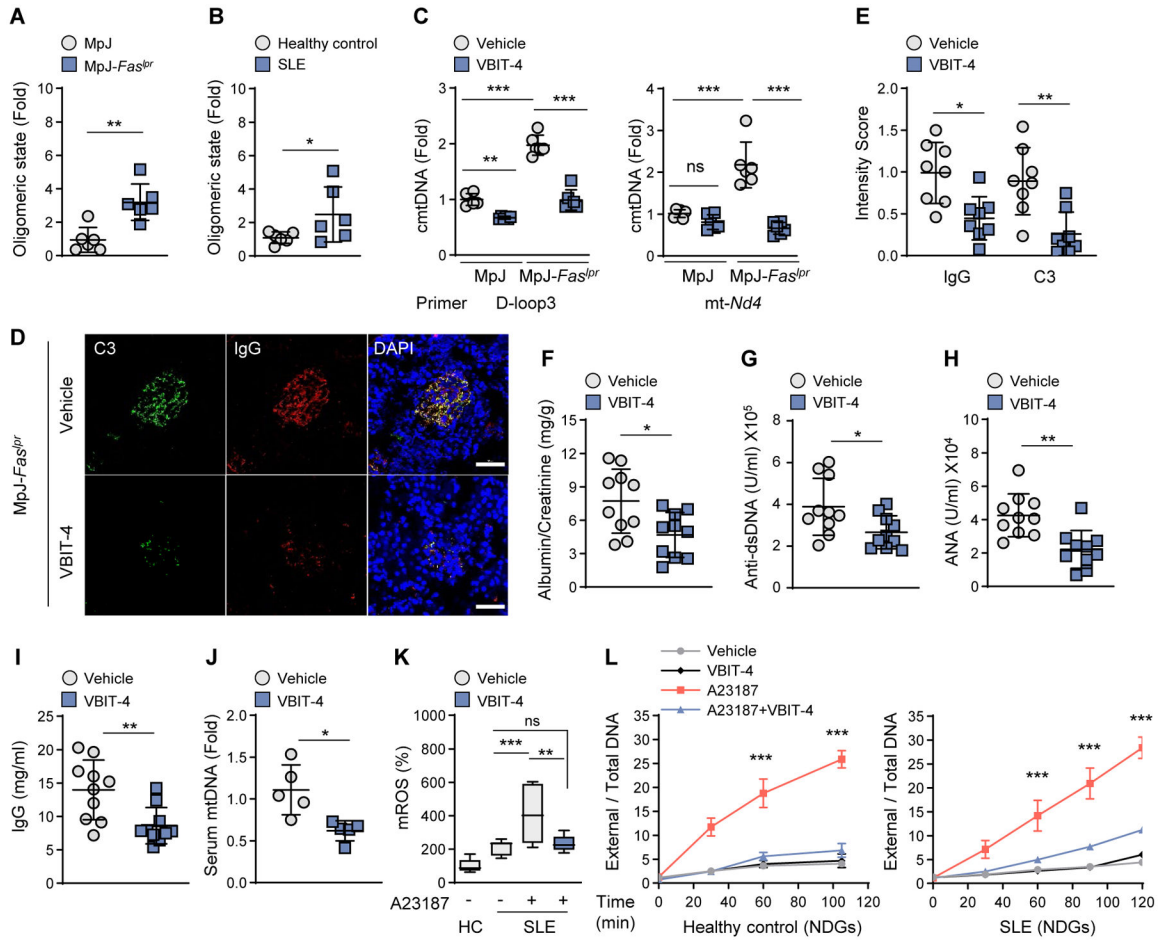
VDAC1. All values are presented as the mean ± SEM of at least three independent experiments. *p < 0.05; **p < 0.01; ***p < 0.005; ns, not significant.

Fig. 4. VDAC1 oligomerization inhibitor VBIT-4 ameliorates lupus-like disease.
(**A**) The formation of VDAC1 oligomers in splenocytes of MRL/MpJ-*Fas^lpr* lupus-prone mice and MRL/MpJ control mice (see fig. S11B; n=6 in each group). (**B**) Oligomeric state of VDAC1 in PBMC of healthy control and SLE patients (see fig. S11C; N=6 in each group). (**C**) cmtDNA levels were measured in splenocytes (A) after treatment with VBIT-4 (10 μM). (**D** and **E**) Kidney glomeruli of VBIT-4-treated mice, stained with antibodies against complement C3 (green) and IgG (red). Nuclei were stained with Hoechst (blue). Scale bars, 20 μm (D). Fluorescence intensity of C3 and IgG in (D) (n=8 in each group) (E). (**F** to **I**) Urinary albumin:creatinine ratio (F), serum anti-dsDNA levels (G), ANA levels (H), and IgG levels (I) of VBIT-4-treated mice (n=10 in each group). (**J**) Serum cell-free mtDNA levels of VBIT-4-treated mice (n=5 in each group). (**K**) mROS levels were measured by mitoSOX in PBMCs of healthy controls (HC) and SLE patients (n = 3 in each group). (**L**) A23187-induced NET formation by NDGs either from HC or SLE subjects was measured by SYTOX-PicoGreen plate assay (n=3 in each group). All values are presented as the mean ± SEM. *p < 0.05; **p < 0.01; ***p < 0.005; ns, not significant.